LCC – 0012, 10/02/99
KEK –aaa-bbb
SLAC – www-xxx

Linear Collider Collaboration Tech Notes

BNS Profiles and Sensitivity of Beam Orbit of the NLC Linac

February 10, 1999

G.V. Stupakov
Stanford Linear Accelerator Center
Stanford, CA, USA

Abstract:
Using the computer program LIAR we simulate different BNS regimes in the main NLC linac. The energy overhead for each regime is determined, and both the orbit sensitivity for a small quadrupole offset, and ATL-type ground motion are calculated. A single bunch emittance growth caused by initial offset, slope and tilt of the bunch is also simulated..

BNS Profiles and Sensitivity of Beam Orbit in the NLC Linac

G. V. Stupakov, SLAC

0.1 BNS Profiles

Using simulation code LIAR [1], we calculated the emittance growth of a single bunch in the NLC linac due to short-range wakefield ($a/\lambda = 0.18$) for the lattice CD1.1 and different BNS profiles.

The main simulation parameters are listed in the following table:

E_0	10	[GeV]
E_f	500	[GeV]
N	$1.1 \cdot 10^{10}$	
$\gamma\epsilon_y$	$4 \cdot 10^{-8}$	[m rad]
$\gamma\epsilon_x$	$3.6 \cdot 10^{-6}$	[m rad]
σ_z	$150 \cdot 10^{-6}$	[m]

The bunch was represented by 20 slices with 1 macroparticle per slice.

Eight different BNS profiles were simulated in which RF phases were switched at two locations in the linac. This approach closely follows the procedure adopted in the ZDR [2]. The energy of the beam E_1 and E_2 at the switch points, and the RF phases ϕ_1 (before the first switch), ϕ_2 (after the first switch), and ϕ_3 (after the second switch) are given in the following table:

Set #	ϕ_1 [deg.]	E_1 [GeV]	ϕ_2 [deg.]	E_2 [GeV]	ϕ_3 [deg.]
1	4	30	-7	445.3	-30
2	8	30	-5	407	-30
3	10	30	-3	380	-30
4	12	30	-1	355	-30
5	14	30	1	331	-30
6	16	30	3	311	-30
7	18	30	5	295	-30
8	20	30	7	280	-30

These parameters where chosen so that the final energy spread of the bunch at the end of the linac, as dictated by the final focus optics, is approximately equal to 0.3%.

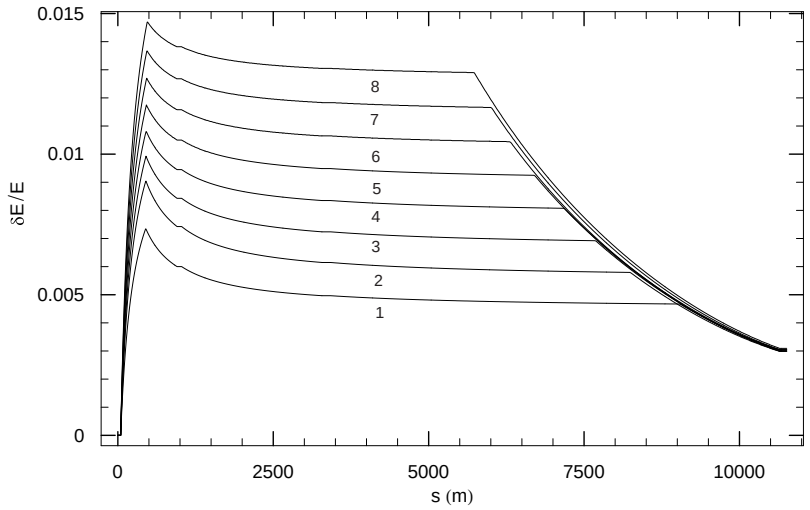

Figure 1: Energy spread profiles for 8 sets of RF phases along the linac. BNS regime is indicated by the number near each curve.

The rms energy spread of the beam as a function of position in the linac is shown in Fig. 1. To characterize the loss of acceleration in each case, we use the *energy overhead* defined as follows. Let $G(s)$ stand for the amplitude of the accelerating gradient as a function of position in the linac, and $\phi(s)$ stand for the RF phase, so that the energy increase of the beam after passing the distance ds is $G(s)\cos\phi(s)\,ds$. The energy E_f at the end of the linac is

$$E_f = E_i + \int_0^L ds\, G(s)\cos\phi(s), \tag{1}$$

where E_i is the initial beam energy, and L is the length of the linac; hence the quantity $\int_0^L ds\, G(s)\cos\phi(s)$ is fixed by the requirement of the given final energy. For a short bunch, the quantity $\int_0^L ds\, G(s)\sin\phi(s)$ is proportional to the correlated energy spread at the end of the linac. It is also fixed by requirement of the energy spread at the end tolerated by the final focus optics. With these two quantities, we define the average RF phase as

$$\langle\phi\rangle = \arctan\left(\frac{\int_0^L ds\, G(s)\sin\phi(s)}{\int_0^L ds\, G(s)\cos\phi(s)}\right), \tag{2}$$

and calculate the energy overhead as

$$\text{BNS overhead} = 1 - \frac{\int_0^L ds\, G(s) \cos\phi(s)}{\cos\langle\phi\rangle \int_0^L ds\, G(s)}\,. \tag{3}$$

This quantity is always nonnegative, and is equal to zero only if $G(s)$ does not depend on s and $\phi(s) = \langle\phi\rangle$. It characterizes the energy loss due to the variation of the RF phase along the linac relative to the constant RF phase profile determined by the given final energy and the final energy spread. In our calculations $\langle\phi\rangle = -10.6^\circ$. The energy overhead for different BNS profiles is shown in Fig. 2.

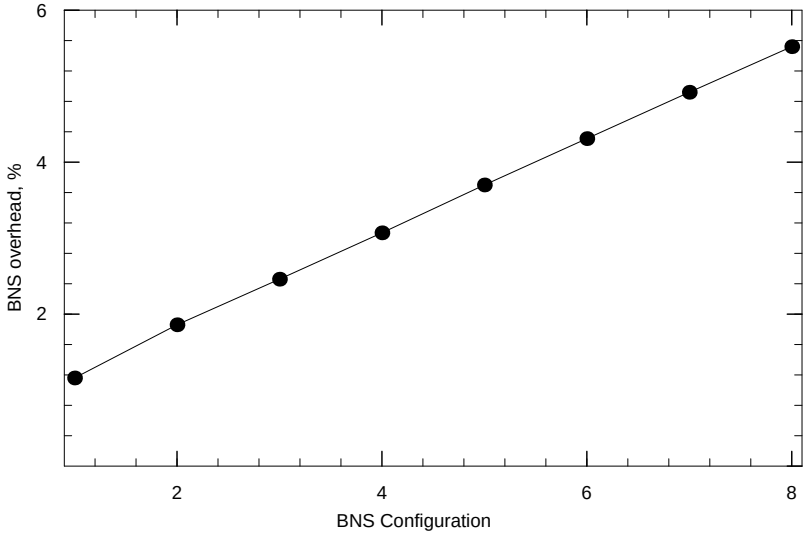

Figure 2: Energy overhead in percentage points for different BNS profiles.

0.2 Orbit Sensitivity

We also calculated the emittance growth of the beam resulting from an offset of a single quadrupole magnet. In this simulation, a focusing (in the vertical plane) quadrupole located at distance s from the beginning of the linac was moved in the vertical direction by 1 micron, and the resulting emittance growth of the beam was calculated as a function of position s. Such curves are plotted in Fig. 3 for different BNS profiles. As we see from this plot,

increasing the strength of the BNS damping generally lowers the sensitivity for a weak-BNS regimes 1 (not shown in the figure), 2 and 3, however, for stronger BNS (regimes 4 through 8) the emittance growth is roughly independent of the BNS configuration. A similar behaviour was observed for

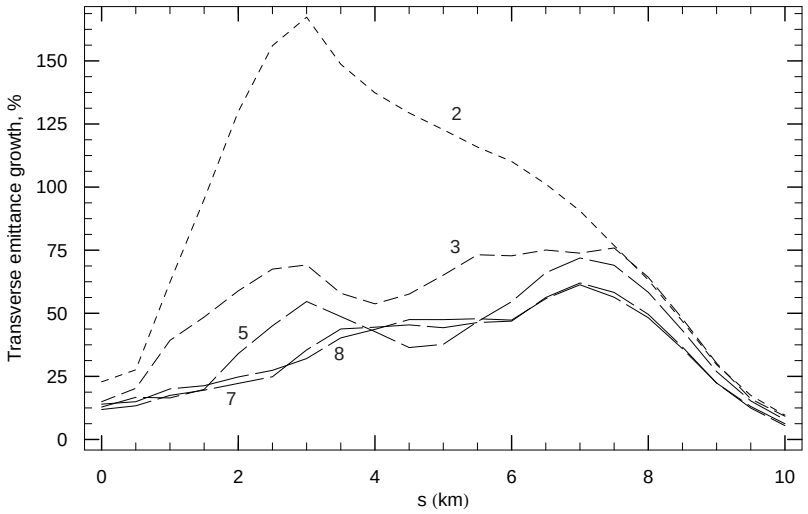

Figure 3: Sensitivity to quad offset for different BNS profiles. The BNS set is shown by a number near the curve.

the emittance growth caused by the ATL-like motion of the lattice elements, Fig. 4. This simulation was performed with the ATL constant equal to 0.5×10^{-6} μm^2/m/s, and the time interval of 30 min. The plot shows the emittance of the beam as a function of the position in the linac. Notice that in these simulations no steering or orbit correction was applied to the beam, which usually dramatically improve the tolerance in this case. In this sense, out result does not reflect the real situation, and is presented here for relative comparison of the effect of different BNS profiles only.

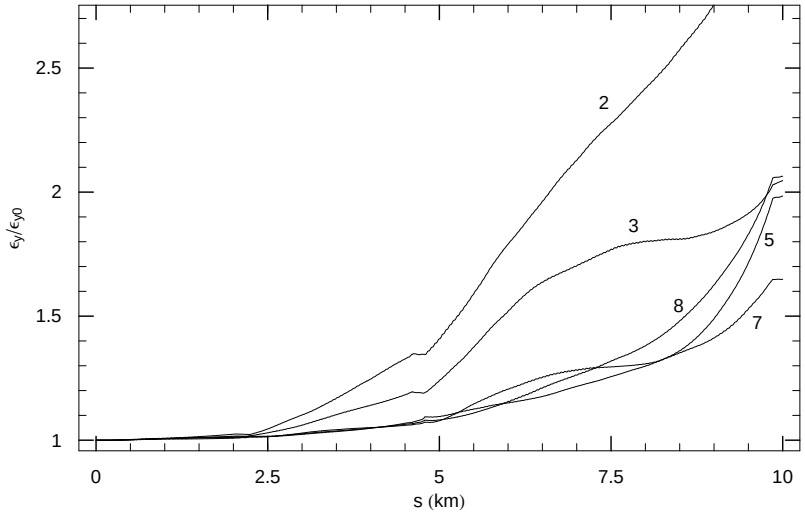

Figure 4: Beam emittance growth due to linac misalignment corresponding to the ATL ground motion after 30 min. The BNS configuration is shown by a number near the curve.

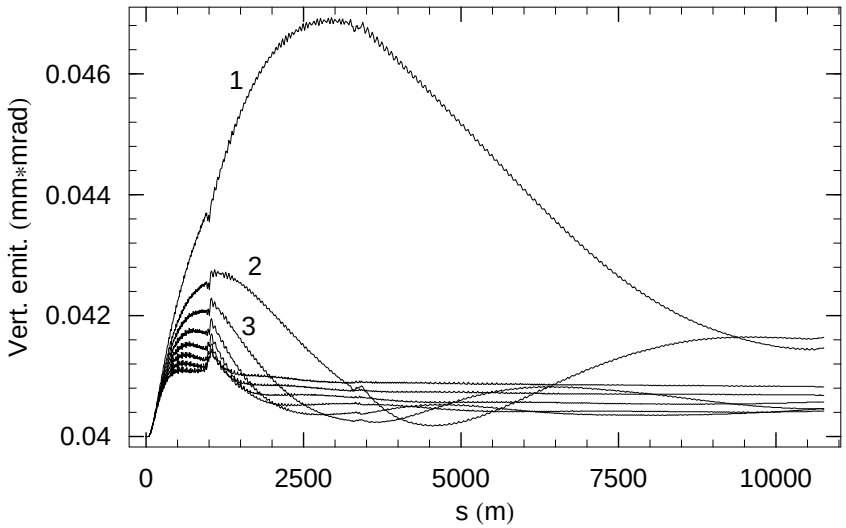

Figure 5: Beam emittance growth due to initial offset of 1 micron. The BNS configuration is shown by numbers near the curves.

We have also simulated the effect of the emittance growth due to a small initial beam offset in the vertical plane, Fig. 5, and an initial orbit angle, Fig. 6. Finally, an initial tilt of the beam was simulated in which the offset of each slice in the bunch is given by $y = \alpha z$, where α is a small angle, and the centroid of the bunch is located on the axis. The emittance growth for $\alpha = 0.01$ rad is shown in Fig. 7. Those simulations show that increasing the BNS energy spread beyond regimes 3 and 4 does not strongly effect the emittance growth.

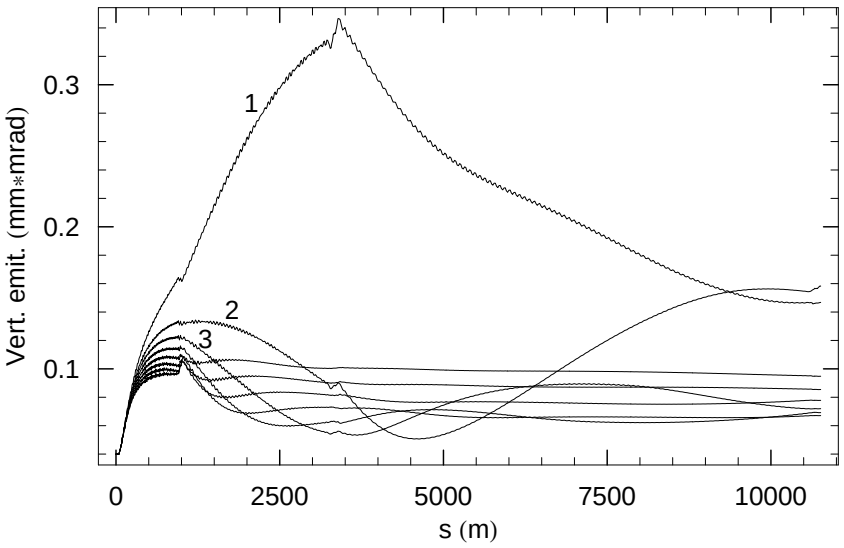

Figure 6: Beam emittance growth due to initial orbit angle of 1 microradian. The BNS configuration is shown by numbers near the curves.

Numerical values for the vertical emittance increase at the end of the linac corresponding to Figs. 5-7 are summarized in the table below. Note that for the last row, the increase of the emittance is calculated relative to the nominal value 4×10^{-8} mm-mrad, although due to the tilt, the actual emittance at the entrance to the linac is somewhat higher (see Fig. 7).

0.3 Conclusion

Using simulation with the computer code LIAR we found the optimal BNS regimes for the NLC main linac. Those regimes correspond to profiles 3 and

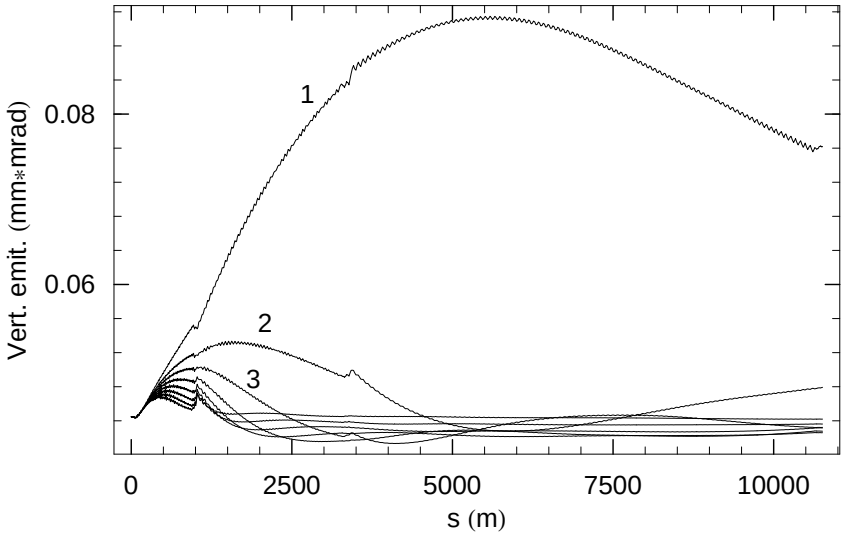

Figure 7: Beam emittance growth due to initial tilt of the bunch of 0.01 rad. The BNS configuration is shown by numbers near the curves.

BNS Regime	1	2	3	4	5	6	7	8
Initial offset, 1 μ	3.7	4.1	1.2	1.1	1.0	1.4	1.7	2.1
Initial slope, 1 μrad	267	295	80	73	68	95	113	137
Initial tilt, 0.01 rad	91	20	8	7	6	8	9	10

Table 1: Emittance increase at the end of the linac in percentage points.

4 in Fig. 1. They will result in the energy overhead around 3%. Further increase of the energy spread of the beam does not essentially suppress the emittance growth of the bunch.

References

[1] R. Assmann et al. "LIAR - A Computer Program for Linear Accelerator Simulations", SLAC/AP-103 (1996).

[2] The NLC Design Group, "Zero-Order Design Report for the Next Linear Collider", SLAC Report 474 (1996).